Snapshots of Crystal Growth: Nanoclusters of Organic Conductors on Au(111) Surfaces

Joachim Hossick Schott and Michael D. Ward*

Contribution from the Department of Chemical Engineering and Materials Science, University of Minnesota, Amundson Hall, 421 Washington Avenue SE, Minneapolis, Minnesota 55455

Received January 14, 1994®

Abstract: Mono- and multilayer crystalline nanoclusters of tetrathiafulvalene–tetracyanoquinodimethane ((TTF)(TCNQ)), a low-dimensional organic conductor in the bulk form, can be formed readily on Au(111) surfaces by vapor phase sublimation under ambient conditions. Scanning tunneling microscopy of monolayer (TTF)(TCNQ) films reveals a two-dimensional density of states (DOS) that is consistent with the arrangement of TTF and TCNQ molecules in the *ac* face of bulk (TTF)(TCNQ), in which the molecular planes are nearly parallel to the Au(111) substrate. In contrast, clusters with thicknesses corresponding to two or three molecular layers exhibit a transformation to a highly anisotropic DOS that can be attributed to interlayer molecular overlap in segregated TTF and TCNQ molecular chains along the *c* axis, which can be described as "molecular wires". The orientation of the crystalline (TTF)(TCNQ) clusters is preserved throughout the crystal growth sequence, leading to meso- and macroscopic (TTF)(TCNQ) needles that are oriented perpendicular to the Au(111) substrate. These studies provide visualization of crystal growth from the initial stages of nucleation to macroscopic crystals and a revealing example of the changes in electronic structure that occur during the evolution of molecular (TTF)(TCNQ) nuclei into a bulk crystalline phase.

Introduction

Molecular crystals containing organic components exhibit a variety of electronic properties, including electrical conductivity, superconductivity, and nonlinear optical behavior.[1] Much of the interest in these materials stems from the ability to employ molecular-level "crystal engineering" strategies,[2] which aim to rationally manipulate crystal packing and, consequently, influence bulk physical and electronic properties. Electrically conductive crystals of organic charge-transfer salts may provide the basis for a new class of molecular-scale devices with physical and electronic characteristics that can be controlled by molecular design.[3] These materials, including the well-known metallic conductor (TTF)(TCNQ) (TTF = tetrathiafulvalene; TCNQ = tetracyanoquinodimethane), typically contain quasi-one-dimensional segregated stacks of donor and/or acceptor molecules that afford highly anisotropic conductivity. While the bulk[4] and surface[5–8] structural properties of macroscopic crystals of (TTF)(TCNQ) have been investigated extensively, the self-assembly, nucleation, and crystallization processes that are responsible for its formation are not well understood. Indeed, little is known about the crystal growth mechanism of low-dimensional conductors on metal surfaces, even though the principal method for the synthesis of these materials is electrochemical crystallization on metal electrodes. Of particular interest are the structural and electronic properties of nanometer size crystal nuclei, and their interaction with the substrate upon which nucleation occurs. Indeed, understanding of the structure and electronic characteristics at the nanometer length scale is crucial if the rational design of molecular-scale devices (e.g., heterojunctions, sensors, photoelectrochemical cells) is to be achieved, as evidenced by several recent studies of epitaxially grown thin organic films on inorganic substrates.[9–13]

Herein we describe the observation, using scanning tunneling microscopy (STM),[14] of nanoscale crystalline nuclei of (TTF)(TCNQ) on Au(111) surfaces and their evolution into bulk (TTF)(TCNQ) crystals. We have discovered that nuclei clusters of monolayer thickness are oriented with the molecular planes parallel to the Au(111) substrate, and that this orientation is preserved throughout the crystal growth process. Furthermore, STM reveals a novel transformation of the electronic structure in which monolayer thick clusters exhibit a two-dimensional density of states (DOS) typical of electronic states localized on individual TTF and TCNQ molecules, whereas clusters consisting of two or three layers exhibit highly anisotropic DOS due to segregated TTF and TCNQ molecular chains that can be described as "molecular wires." These studies provide visualization of a transition from localized to bulk electronic structure in an organic conductor.

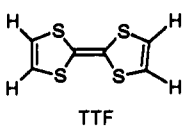

TTF

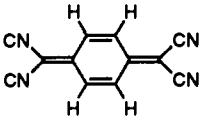

TCNQ

Experimental Section

Single crystals of (TTF)(TCNQ) for preparation of the nanoclusters were synthesized by combining equimolar amounts of TTF and TCNQ

* Author to whom correspondence should be addressed.

® Abstract published in *Advance ACS Abstracts*, June 15, 1994.

(1) (a) Miller, J. S.; Epstein, A. J.; Reiff, W. M. *Science* **1988**, *240*, 40. (b) Miller, J. S. *Extended Linear Chain Compounds*; Plenum: New York, 1982–3; Vol. 1–3. (c) Garito, A. F.; Heeger, A. J. *Acc. Chem. Res.* **1974**, *7*, 232. (d) Torrance, J. B. *Acc. Chem. Res.* **1979**, *12(3)*, 79. (e) Zyss, J.; Tsoucaris, G. *Structure and Properties of Molecular Crystals*; Pierrot, M., Ed.; Elsevier: Amsterdam, 1990; pp 297–350.

(2) (a) Schmidt, G. M. J. *Pure Appl. Chem.* **1971**, *27*, 647. (b) Desiraju, G. *Crystal Engineering—The Design of Organic Solids*; Elsevier: New York, 1989. (c) Lehn, J. M. *Angew. Chem., Int. Ed. Engl.* **1988**, *27*, 89. (d) Fagan, P. J.; Ward, M. D.; Calabrese, J. C. *J. Am. Chem. Soc.* **1989**, *111*, 1698.

(3) Carter, F., Ed. *Molecular Electronic Devices*; Marcel Dekker: New York 1982.

(4) Kistenmacher, T. J.; Philipps, T. E.; Cowan, D. O. *Acta Crystallogr.* **1973**, *B30*, 763.

(5) Sleator, T.; Tycko, R. *Phys. Rev. Lett.* **1988**, *60*, 1418.

(6) Pan, S.; deLozanne, A. L.; Fainchtein, R. *J. Vac. Sci. Technol.* **1991**, *B9*, 1017.

(7) Bar, G.; Magonov, S. N.; Cantow, H. J.; Gmeiner, J.; Schwoerer, M. *Ultramicroscopy* **1992**, *42–44*, 644.

(8) Nakajima, K.; Kageshima, M.; Ara, N.; Yoshimura, M.; Kawazu, A. *Appl. Phys. Lett.* **1993**, *62*, 1892.

(9) Nebesny, K. W.; Collins, G. E.; Lee, P. A.; Chau, L. K.; Danziger, J. L.; Osburn, E.; Armstrong, N. R. *Chem. Mater.* **1991**, *3*, 829.

(10) Tada, H.; Sakai, K.; Komo, A. *Jap. Appl. Phys.* **1991**, *30*, L306.

(11) (a) Chau, L. K.; England, C. D.; Chen, S.; Armstrong, N. R. *J. Phys. Chem.* **1993**, *97*, 2699. (b) Möbus, M.; Karl, N.; Kobayashi, T. *J. Cryst. Growth* **1992**, *116*, 495.

(12) Li, Y. Z.; Chander, M.; Patrin, J. C.; Weaver, J. H.; Chibante, L. P. F.; Smalley, R.E. *Science* **1991**, *253*, 429.

0002-7863/94/1516-6806$04.50/0

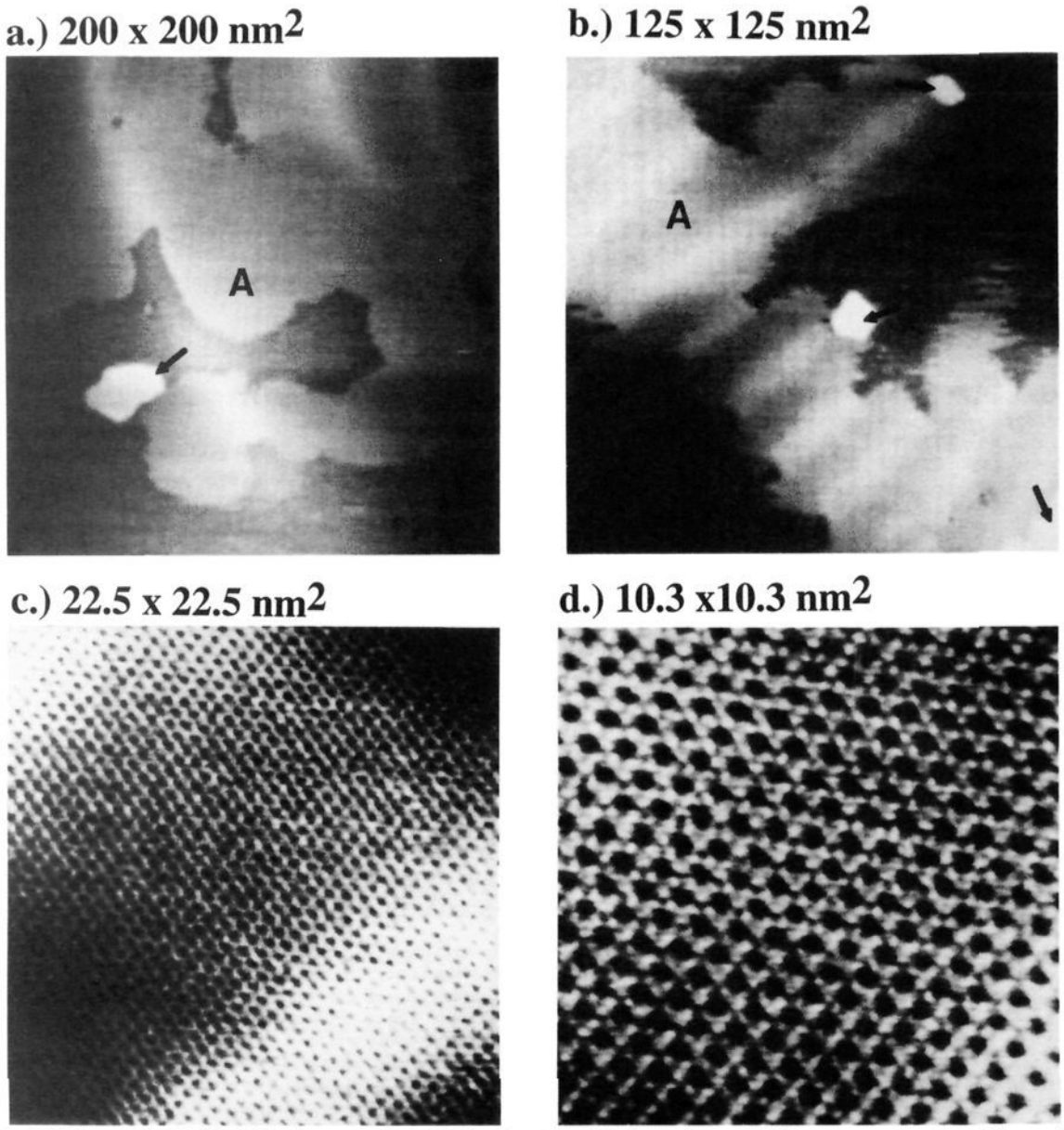

Figure 1. STM images of (TTF)(TCNQ) clusters on the Au(111) surface. (a and b) Large clusters exhibit a pattern of varying brightness in STM which is reminiscent of a Moiré pattern. On the cluster shown in part b the pattern is regular. The small, bright areas indicated by arrows in both images are attributed to gold islands, based on the 2.9-Å step-height at the edge of the islands. Similarly, the bright area in the lower right corner of the image in part b is attributed to a monoatomic Au step. (c) Section of the cluster shown in part b. (d) STM image revealing the molecular architecture within the cluster. Bias voltage (V_b) and tunneling current (i_t): (a) –175 mV, 0.1 nA; (b, c, d) –195 mV, 0.15 nA. All images are low pass filtered once.

in acetonitrile, followed by recrystallization from acetonitrile. Au(111) surfaces were prepared according to a previously described procedure.[15-17] One end of a ~2-cm piece of Au wire (99.999% purity, 0.5-mm diameter, Johnson Matthey) was melted in a hydrogen–oxygen flame to form a sphere of 1–2-mm diameter. Upon cooling the sphere in air, highly reflective facets appear and prove to be atomically flat in STM. Since the samples were not further annealed, the facets exhibited the unreconstructed phase of the Au(111) surface. Nanoclusters of (TTF)-(TCNQ) on the Au(111) substrate were fabricated by exposure of freshly prepared Au(111) surfaces to (TTF)(TCNQ) vapor for 5 min. This was accomplished by positioning the substrate surface ~5 mm above (TTF)-(TCNQ) crystals at room temperature and ambient pressure. Crystals of meso- and macroscopic dimensions (~0.1 to ~100 μm^3) were grown on the Au(111) substrates by evaporation of (TTF)(TCNQ) at slightly elevated temperatures (60 °C) and/or for time periods of up to ~15 h. STM data were acquired in ambient air using a Nanoscope II scanning tunneling microscope equipped with mechanically cut Pt(90%)Ir(10%) tips. The tip was held at virtual ground and the bias voltage was applied to the sample. Data were collected in the constant current mode. On the basis of images of Au(111) surfaces, the lateral accuracy of individual atom positions is ≤±0.3Å. All images consist of 400 × 400 data points and were obtained with a scan rate of 8.6 Hz.

Results and Discussion

Brief exposure of Au(111) surfaces to (TTF)(TCNQ) vapor under ambient conditions resulted in the formation of irregularly shaped, large (≈10^4 nm^2) two-dimensional clusters on the Au substrate that can be observed readily by STM (Figure 1, regions A). The apparent average height of these clusters, with respect to the gold surface, was 1.5 Å. While this apparent height is less

(13) Li, Y. Z.; Chander, M.; Patrin, J. C.; Weaver, J. H.; Chibante, L. P. F.; Smalley, R. E. *Science* **1991**, *252*, 547.
(14) Binnig, G.; Rohrer, H.; Gerber, Ch.; Weibel, E. *Phys. Rev. Lett.* **1982**, *49*, 57.
(15) Hossick Schott, J.; White, H. S. *Langmuir* **1992**, *8*, 1955.
(16) Hossick Schott, J.; Arana, C. R.; Abruña, H. D.; Petach, H. H.; Elliott, C. M.; White, H. S. *J. Phys. Chem.* **1992**, *96*, 5223.
(17) Hsu, T.; Cowley, T. M. *Ultramicroscopy* **1983**, *11*, 125.

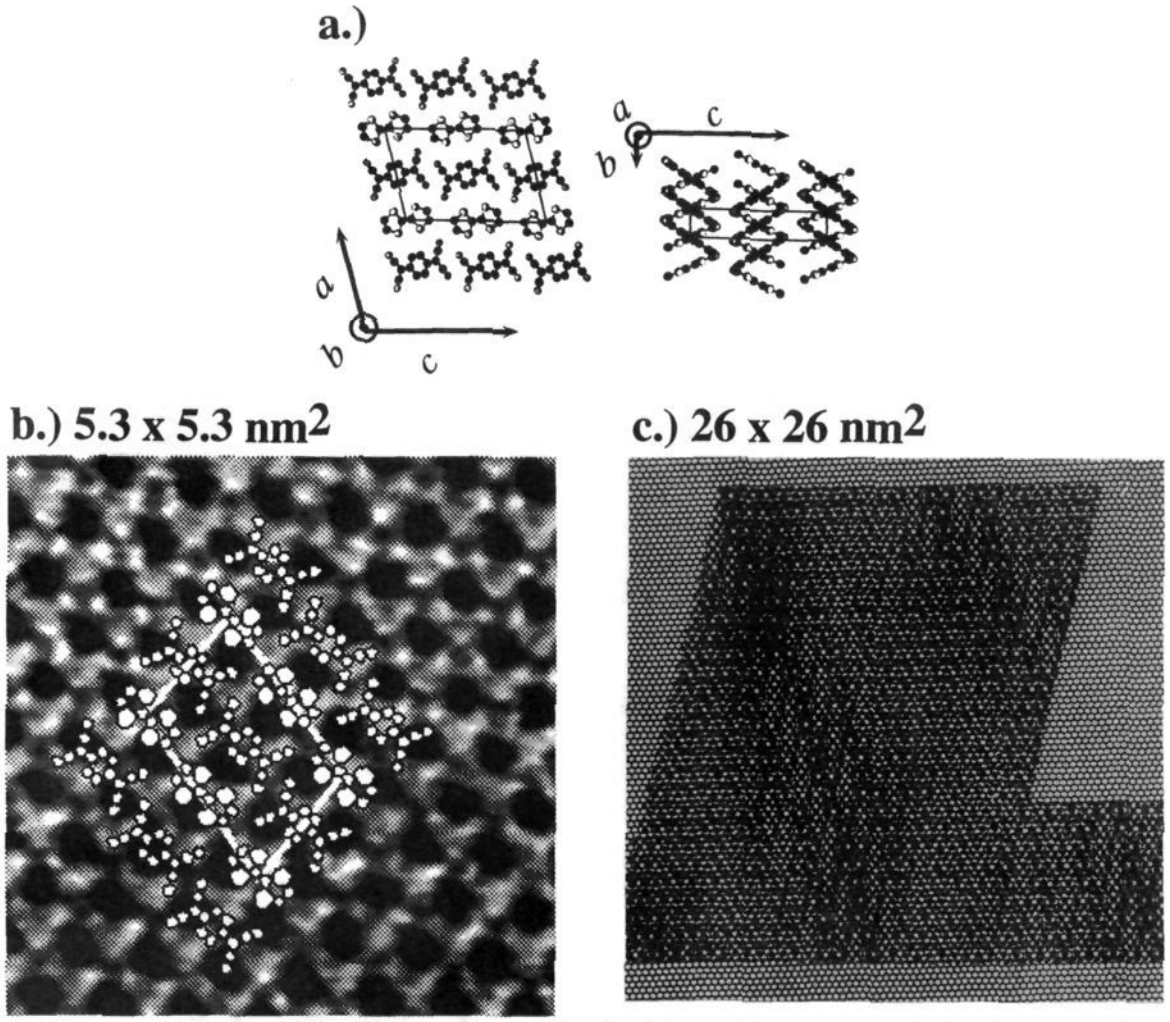

Figure 2. (a) The *ac* and the *bc* face of (TTF)(TCNQ) as determined from the single-crystal X-ray structure, with the unit cell indicated. Note that the *bc* face represents a side view of the (TTF)(TCNQ) stacks. (b) Superposition of the molecular motif of the (TTF)(TCNQ) *ac* plane, obtained from the single-crystal X-ray structure, on a section of the STM data of Figure 1d. The *ac* unit cell, indicated by the white outline, is arranged in an azimuthal orientation in which the unit cell dimensions agree with the tunneling current contrast. The translational position of the *ac* unit cell, with respect to the STM data, was chosen arbitrarily as TTF and TCNQ molecules could not be unambiguously distinguished from the STM tunneling contrast. (c) Model of the Moiré pattern generated by superposition of a *ac* monolayer sheet on the Au(111) lattice. The periodicity of the pattern depicted here is approximately 15 nm, similar to that of the pattern in Figure 1b. The crystal structure of (TTF)(TCNQ) was retrieved from the Cambridge Crystal Structural Database (Cambridge Crystallographic Data Centre, University Chemical Library, Cambridge, England, Version 5.05, update April 1993) using the Tektronix CAChe Molecular Modeling System.

than the molecular thickness of TTF or TCNQ (≈3.8 Å), this observation can be attributed to the electronic properties that result from the combined density of states of the monolayer and the substrate (see below). It is important to note that these clusters were only observed when the Au substrate was exposed to the (TTF)(TCNQ) charge-transfer salt; identical experiments attempted separately with TTF or TCNQ did not afford these features. We refer to these clusters as Type I; occasionally 100–200 Å long needle-shaped clusters were observed in which, based on the tunneling current contrast, the TTF and TCNQ stacking axes were parallel to the substrate. A detailed description of these clusters, which are designated as Type II clusters, is deferred to a future publication.[18]

The tunneling current contrast at higher resolution is consistent with a single layer of (TTF)(TCNQ) molecules arranged in a motif identical to that of the *ac* plane of a bulk (TTF)(TCNQ) crystal (Figure 2a,b).[4] This orientation would require that the TTF and TCNQ planes are parallel (or nearly so) to the Au (111) substrate, similar to behavior commonly exhibited by large aromatic molecules.[9,10,19–21] The lattice constants determined from the periodicity of tunneling current contrast (a = 11.0 ± 1 Å, c = 16.5 ± 1 Å, β = 104° ± 1°) are similar to those of the *ac* plane obtained from the single-crystal X-ray structure (monoclinic $P2_1/c$, a = 12.298 Å, b = 3.819 Å, c = 18.468 Å, β = 104.46°).[4] However, it is evident that the a and c lattice parameters are smaller in the STM data. While this may be partially attributable to intrinsic measurement error that is common for room temperature STM data (± 5–10%), it is also reasonable to suggest that a single molecular layer will pack more densely than in the bulk material in order to compensate for the absence of van der Waals interactions between the *ac* molecular layers. It should be noted that individual TTF and TCNQ molecules could not be unambiguously distinguished from the STM tunneling contrast. This is not entirely unexpected, as recent

(18) Hossick Schott, J.; Ward, M. D. Submitted for publication.

(19) Collins, G. E.; Nebesny, K. W.; England, C. D.; Chau, L. K.; Lee, P. A.; Parkinson, B. A.; Armstrong, N. R. *J. Vac. Sci. Technol.* **1992**, *A10*, 2902.

(20) Hara, M.; Sasabe, H.; Yamada, A.; Garito, A. F. *Jap. Appl. Phys.* **1989**, *28*, L306.

(21) Collins, G. E.; Williams, V. S.; Chau, L. K.; Nebesny, K. W.; England, C.; Lee, P. A.; Lowe, T.; Fernando, Q.; Armstrong, N. R. *Synth. Met.* **1993**, *54*, 351.

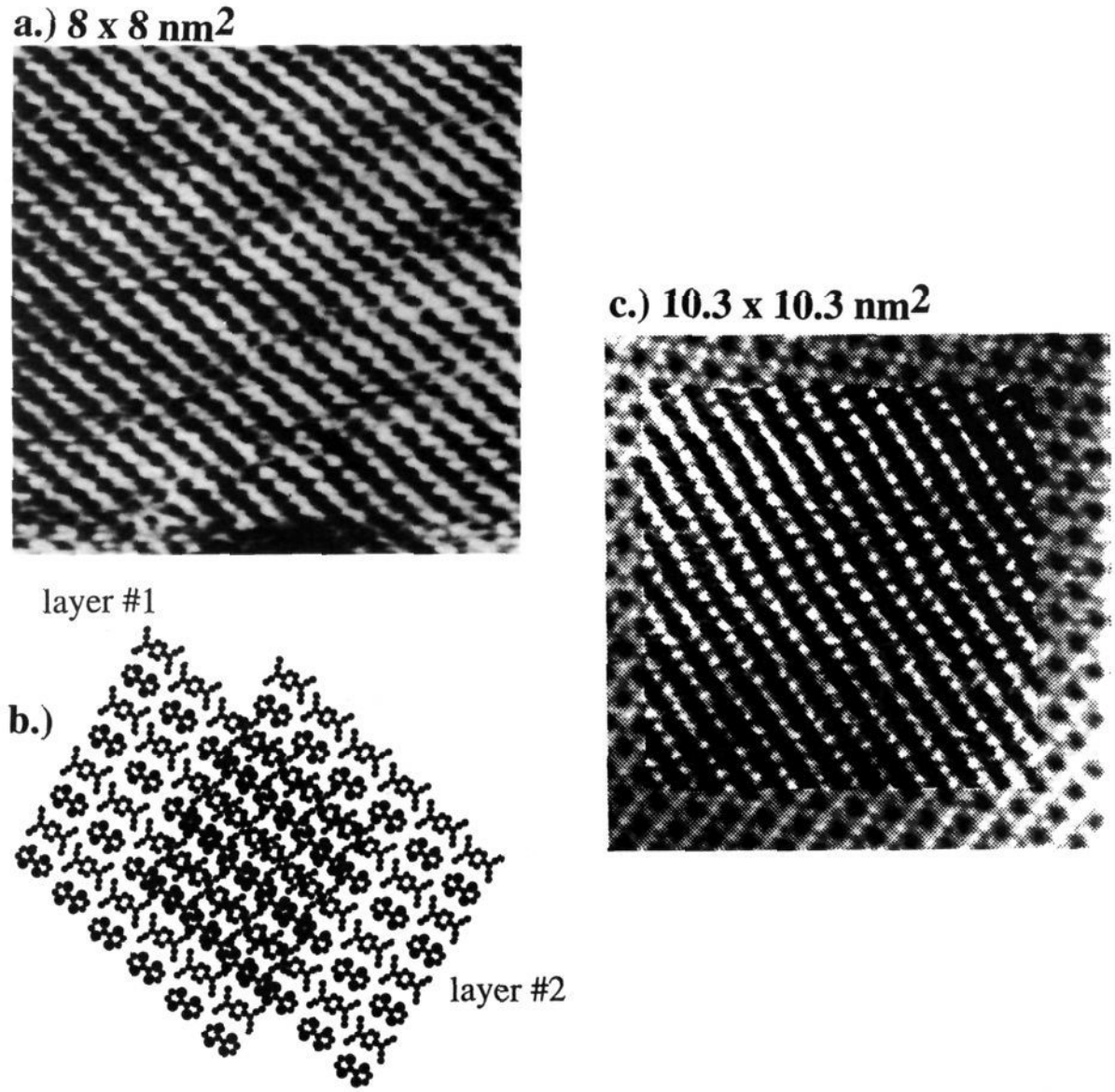

Figure 3. (a) Low pass filtered STM image of a molecular *ac* multilayer, which exhibits tunneling current contrast associated with molecular ribbons. The spacing between neighboring ribbons is 5 ± 1 Å, which is approximately equal to $a/2$ (=6.2 Å). $V_b = -228$ mV, $i_t = 0.17$ nA. (b) Molecular model of two superimposed *ac* monolayer sheets related by a $c/4$ translation, simulating the $c/4$ translation of the molecules in layer $n + 1$ with respect to layer n. Note that each molecule in the upper layer overlaps only partially with the molecule in the layer beneath, resulting in imaging of segregated, electronically continuous TTF and TCNQ ribbons along the c axis. The distance between neighboring ribbons is $a/2$. (c) Computer generated superposition of two STM images from the same molecular *ac* monolayer obtained after a $c/4$ glide symmetry operation of one of the layers. The c axis was assigned based on the relationship of the tunneling current to the *ac* lattice parameters (Figure 2b).

STM investigations of simple adsorbates (benzene, Xe atoms) on single-crystal metal surfaces have demonstrated the difficulties relating tunneling features to the structure of the adsorbates.[22]

The STM data also display large scale corrugations in the tunneling current with typical periodicities of 150–200 Å (Figure 1a,b). The source of these corrugations is suggested by superposition of a molecular model of the (TTF)(TCNQ) *ac* plane on the hexagonal Au(111) lattice, which yields a Moiré pattern closely resembling the tunneling current corrugations observed in the STM images (Figure 2c). Different experimentally observed (TTF)(TCNQ) clusters exhibit Moiré patterns with varying periodicity and regularity, which can be simulated simply by rotation and translation of the lattice models. This clearly indicates that the (TTF)(TCNQ) clusters do not exhibit preferred azimuthal orientations with respect to the Au(111) substrate, as may be expected from the poor commensurability of the (TTF)-(TCNQ) and the Au(111) lattices. The apparent height of the clusters in the *valley* of the Moiré hill and valley structure is only 1.3 Å. The small value of the apparent height and the observation of the Moiré patterns, which result from superposition of the (TTF)(TCNQ) and Au(111) wave functions, strongly substantiate a monolayer thickness for the (TTF)(TCNQ) clusters. Furthermore, the perturbation of the local DOS of the (TTF)-(TCNQ) monolayer by the metal wave functions evident from the Moiré patterns may be partially responsible for the inability to assign the features to individual TTF and TCNQ molecules.

Exposures of the Au(111) surface to (TTF)(TCNQ) vapor for longer times resulted in clusters which, based on comparison to the monolayer clusters, have thicknesses corresponding to two or three molecular layers. In contrast to the monolayer clusters, these regions exhibited a ribbon motif with an interribbon distance of 5 ± 1 Å, approximately equivalent to $a/2$ (Figure 3a). The

(22) (a) Weiss, P. S.; Eigler, D. M. *Phys. Rev. Lett.* **1993**, *71*, 3139. (b) Eigler, D. M.; Weiss, P. S.; Schweizer, E. K.; Lang, N. D. *Phys. Rev. Lett.* **1991**, *66*, 1189.

reason for this behavior may be explained by considering the molecular overlap of TTF and TCNQ molecules between *ac* layers along the stacking axis, as deduced from the single-crystal X-ray structure. Within the segregated stacks, TTF and TCNQ molecules exhibit "ring-over-bond" overlaps in which adjacent molecules are slipped with respect to each other along their long molecular axes by approximately $c/4$, where c is the lattice direction (Figure 3b). Previous theoretical studies indicate that this motif provides optimal interaction between the molecules along the stacking direction.[23] Accordingly, the spatial distribution of the electronic states associated with TTF and TCNQ molecules in layer $n+1$ will shift by $c/4$ with respect to molecules in layer n, when viewed normal to the molecular planes. Notably, the experimentally observed STM ribbon motif in Figure 3a can be replicated by adding the numerical contrast values of two *ac* layers, in which one of the layers is translated by $c/4$ (Figure 3c). This strongly suggests that the anisotropic tunneling current observed for multilayer clusters is due to a $c/4$ translational relationship between the molecules of adjacent *ac* layers, which results in enhanced intermolecular overlap between TTF and TCNQ molecules and in greater continuity of the DOS along the *c* direction, but with negligible change in the interribbon overlap and DOS along the *a* axis. This results in a pronounced anisotropy of the DOS associated with the *c*-oriented chains, which can be properly described as "molecular wires".

Of particular interest to us is whether crystal characteristics such as morphology, phase, and orientation are preserved throughout the entire crystal growth sequence, from nuclei to macroscopic crystals. Substrate–nuclei interactions and crystal surface energies may be expected to dominate at small length scales, whereas at macroscopic length scales volume free energies can become more significant. Interestingly, prolonged exposure of the Au(111) substrate to (TTF)(TCNQ) results in the formation of highly oriented (TTF)(TCNQ) needles, with their *b* axes (the molecular stacking direction) normal to the substrate. This is evident from scanning electron micrographs at the 10-μm scale as well as from simple visual inspection of the gold substrate (Figure 4). This clearly demonstrates that the orientation of the (TTF)(TCNQ) nanoclusters is preserved throughout the growth process, and indeed is responsible for the growth orientation of the macroscopic crystals. It is interesting to note that rectangular step features are readily evident on the walls of the mesoscopic (TTF)(TCNQ) needles. This is consistent with the presence of the low energy *ab* and *bc* faces, which under the monoclinic symmetry of the crystal are expected to exhibit step angles of 90°. It is also significant that under these conditions the majority of the Au(111) surface is bare, indicating that crystal growth on existing nucleation centers is highly favorable. This observation, and the rather large area occupied by the clusters (by STM standards), is consistent with rapid surface diffusion of (TTF)(TCNQ) on Au(111).

In a limited survey of other organic conductors, we have found that (TTF)(TCNQ) is favorably disposed toward the formation of the two-dimensional nanoclusters. Similar experiments with the organic semiconductor Li^+TCNQ^- result in the *exclusive* formation of the aforementioned Type II clusters, which are observed only occasionally for (TTF)(TCNQ). Molecularly resolved STM images of the Type II (TTF)(TCNQ) and Li^+TCNQ^- clusters reveal that the TCNQ stacking axis in these clusters is oriented parallel to the gold substrate. Since the (TTF)(TCNQ) Type II clusters are observed only on rare occasions, the relationship between their orientation and that of the corresponding mature crystals cannot be discerned. However, microscopic Li^+TCNQ^- crystals observed in scanning electron microscopy are aligned with their needle axes parallel to the Au surface (Figure 4c) and with azimuthal orientation conforming to the 3-fold symmetry of the Au(111) substrate lattice as evidenced by the angles of 60° and 120° between neighboring needles, identical to the orientation of the Li^+TCNQ^- clusters on the molecular scale. Therefore, orientation of the Type II clusters also is preserved during growth from the nanoscopic to the microscopic length scale. The observation of preferred azimuthal orientation for the Type II clusters suggests stronger substrate–nuclei interactions than for the Type I clusters. A detailed description of the Type II clusters will be presented elsewhere.[18]

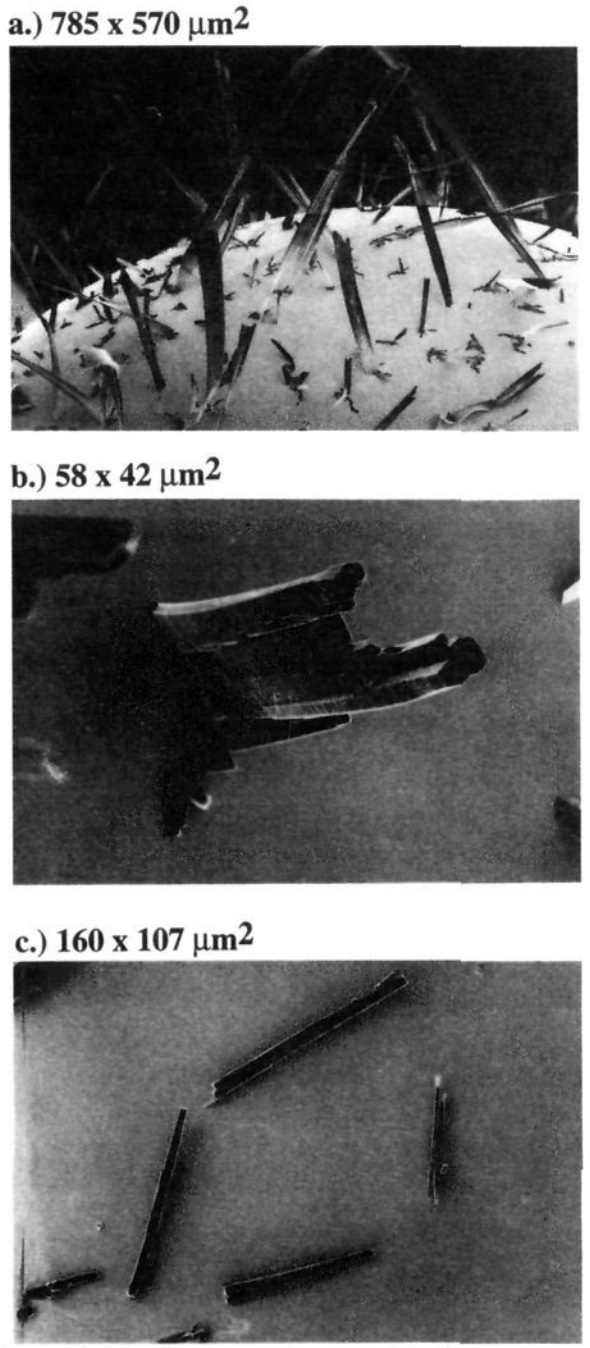

Figure 4. (a) Scanning electron micrograph of the (111) facet area of an Au sphere exposed to (TTF)(TCNQ) vapor at 60 °C. Crystalline (TTF)(TCNQ) columns were grown perpendicular to the Au surface plane. (b) Tilted top view of one of the columns. Note the rectangular step features on the side of the columns, which are expected for *ab* and *bc* (TTF)(TCNQ) crystal faces. (c) Li^+TCNQ^- crystals formed from exposure of a Au(111) substrate to Li^+TCNQ^-. The needle-like crystals are aligned parallel to the surface and exhibit azimuthal orientation with respect to the 3-fold symmetry of the substrate lattice.

(23) Lowe, J. P. *J. Am. Chem. Soc.* **1980**, *102*, 1262.

Conclusions

These STM studies provide revealing insights into the molecular self-assembly process involved in heterogeneous nucleation of (TTF)(TCNQ), particularly with regard to orientation and the transformation between monolayer and multilayer nuclei. The orientation of macroscopic crystals clearly results from the initial formation of two-dimensional nanoclusters, with the orientation preserved throughout the growth process. We anticipate that further studies of the nucleation and growth of organic crystals on well-defined substrates, at the nanoscale level, will provide the fundamental understanding required for control of these processes and fabrication of devices based on these materials.

Acknowledgment. The authors gratefully acknowledge the support of the Office of Naval Research.